Piezoelectric Field Effect Transistor and Nanoforce Sensor Based on a Single ZnO Nanowire

Xudong Wang,[†] Jun Zhou,[†,‡] Jinhui Song,[†] Jin Liu,[†] Ningsheng Xu,[‡] and Zhong L. Wang*,[†]

School of Materials Science and Engineering, Georgia Institute of Technology, Atlanta, Georgia 30332-0245, and School of Physics and Engineering, State Key Lab of Optoelectronic Materials and Technologies, SunYat-Sen (Zhongshan) University, Guangzhou, 510275, China

ABSTRACT

Utilizing the coupled piezoelectric and semiconducting dual properties of ZnO, we demonstrate a piezoelectric field effect transistor (PE-FET) that is composed of a ZnO nanowire (NW) (or nanobelt) bridging across two Ohmic contacts, in which the source to drain current is controlled by the bending of the NW. A possible mechanism for the PE-FET is suggested to be associated with the carrier trapping effect and the creation of a charge depletion zone under elastic deformatioin. This PE-FET has been applied as a force/pressure sensor for measuring forces in the nanonewton range and even smaller with the use of smaller NWs. An almost linear relationship between the bending force and the conductance was found at small bending regions, demonstrating the principle of nanowire-based nanoforce and nanopressure sensors.

Quasi-one-dimensional ZnO semiconducting nanostructures, such as nanowires (NWs) and nanobelts (NBs),[1] are considered as an important multifunctional building block for fabricating various nanodevices. Owing to their unique electronic, optical, and piezoelectric properties,[2] ZnO NWs/NBs have been successfully applied in field effect transistors,[3] light-emitting diodes,[4] laser diodes,[5] sensors,[6] resonators,[7] and piezoelectric devices.[8] Most importantly, ZnO exhibits both semiconducting and piezoelectric properties.[9] The coupling of these two properties endows it with very unique advantages and novel applications. The demonstration of aligned ZnO NW based nanogenerator is a successful example of its kind.[8]

Among all of the nanodevices, the field effect transistor (FET) is one of the most studied systems[10] since it not only is a basic electronic device[11,12] but also exhibits a broad range of applications such as in sensors[13,14] and optoelectronic devices.[15,16] A typical NW FET is composed of a semiconducting NW that is connected by two electrodes at the ends and is placed on a silicon substrate covered by a thin layer of gate oxide. A third electrode is built on the top or bottom of the NW as the gate electrode. The electric signal output from the drain electrode of the NW is controlled by a gate voltage applied between the gate and the NW. An NW-based sensor is a source−drain structured NW FET without a gate; thus, a large portion of the NW is exposed to the environment. The mechanism of NW sensors for sensing gases, biomolecules, or even virus relies on the creation of a charge depletion zone in the semiconductor NW by the surface-adsorbed sensing targets.[17]

In this paper, we report an alternative design of a NW FET without using the gate electrode. With connection of a ZnO NW across two electrodes that can apply a bending force to the NW, the electric field created by piezoelectricity across the bent NW serves as the gate for controlling the electric current flowing through the NW. This piezoelectric field effect transistor (PE-FET) can be considered as a new type of FET, which can be turned on/off by applying mechanical force. As a result, it has been demonstrated as force sensor for measuring forces in the nanonewton range and even smaller.

The experimental design is shown in Figure 1a, and the experimental measurement was carried out in situ in the chamber of a scanning electron microscope (SEM). Inside the SEM chamber, an $x-y$ mechanical stage with a fine moving step of ∼20 nm was located beside the SEM sample stage. The mechanical stage can be controlled independently from the outside of the SEM. A tungsten needle with a machined and polished tip was attached on the stage and connected to the positive electrode of an external power

* Corresponding author. E-mail: zhong.wang@mse.gatech.edu.
† School of Materials Science and Engineering, Georgia Institute of Technology.
‡ School of Physics and Engineerin, State Key Lab of Optoelectronic Materials and Technologies, SunYat-Sen (Zhongshan) University.
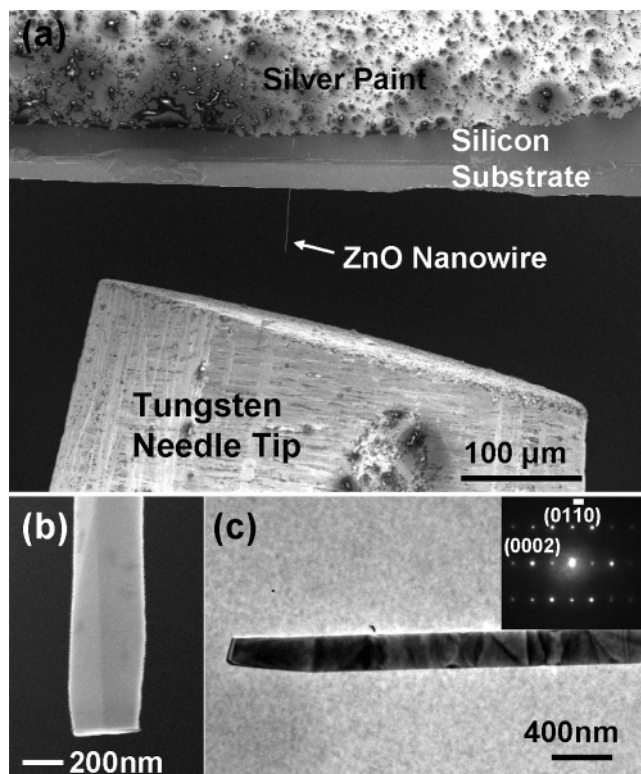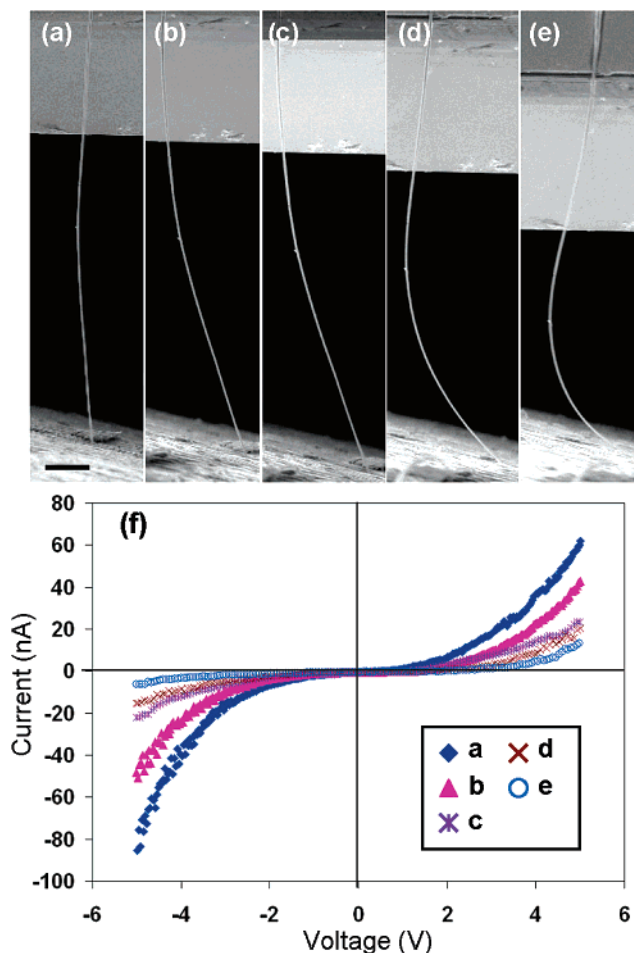
Figure 1. (a) A low-magnification SEM image showing the setup for the in situ measurements. (b) A higher magnification SEM image showing the clean tip of the ZnO nanowire. (c) A TEM image of a ZnO nanowire with single-crystal structure and growth direction [0001]; inset is the corresponding electron diffraction pattern.

Figure 2. (a−e) SEM images with the same magnification showing the five typical bending cases of the ZnO nanowire; the scale bar represents $10\ \mu$m. (f) Corresponding I−V characteristics of the ZnO nanowire for the five different bending cases. This is the I−V curve of the piezoelectric field effect transistor (PE-FET).

source. ZnO NWs were synthesized by the well-established technique of thermal evaporation in a tube furnace.[18] A single NW sample was prepared by aligning the NW on the edge of a silicon substrate using a probe station. The extended length of the NW was $\sim$100 μm, while the other side of the NW was fixed onto the silicon substrate by conductive sliver paint, through which the NW was connected to the negative electrode of the power source. The silicon substrate was placed on the sample stage with the NW pointing at the tungsten needle tip. Both the silver paint and W have Ohmic contact with ZnO.[8] When the required vacuum was achieved in the SEM chamber, the tungsten needle tip was first moved to the center of the image screen. The ZnO NW was then controlled to approach the needle tip by controlling the SEM stage. Focusing the NW and the needle tip at the same time guaranteed that they were aligned at the same height level.

Before contact was made, the ZnO NW was examined under the SEM at a higher resolution. The length of the suspension part of the NW was 88.5 μm. As shown in Figure 1b, the NW's tip was flat and clean and the faceted side surfaces could be clearly observed. The width of this NW was measured to be 370 nm. TEM analysis revealed the single-crystal structure of the ZnO NW and the growth direction was along [0001] (Figure 1c).

In order to achieve a good electrical contact between the ZnO NW and the tungsten tip, a field emission process was introduced at the first stage to clean the NW tip and welding the connection. During the field emission, the ZnO NW was

kept $\sim$10 μm away from the tungsten surface, where 400 V was applied. Under this condition, the emission current could reach as high as $\sim$1 μA.[19] After 1 min of emission, the high voltage was turned off and the ZnO NW was quickly moved toward the tungsten surface to make a contact. We have repeated this process many times and found that it is very effective for making the Ohmic contact, possibly due to the high temperature generated at the tip by the emission process as well as the desorption of the surface contaminant.

The first contact of the NW with the W tip is shown in Figure 2a, where the NW was already bent a little bit because a pushing force was necessary for a good electrical contact. Then, the electron beam of the SEM was turned off and the I−V characteristic was measured by sweeping the voltage from −5 to 5 V. This is to eliminate the effect from the electron beam in SEM. After the measurement, the electron beam was turned back on again, and the NW was bent further by moving the SEM stage in-situ under direct imaging. The bending of the NW was recorded. Following such a procedure, a sequential measurement was carried out. The five typical bending curvatures of the ZnO NW are shown in panels a−e of Figure 2, and their corresponding I−V curves are presented in Figure 2f,. The symmetric shape of
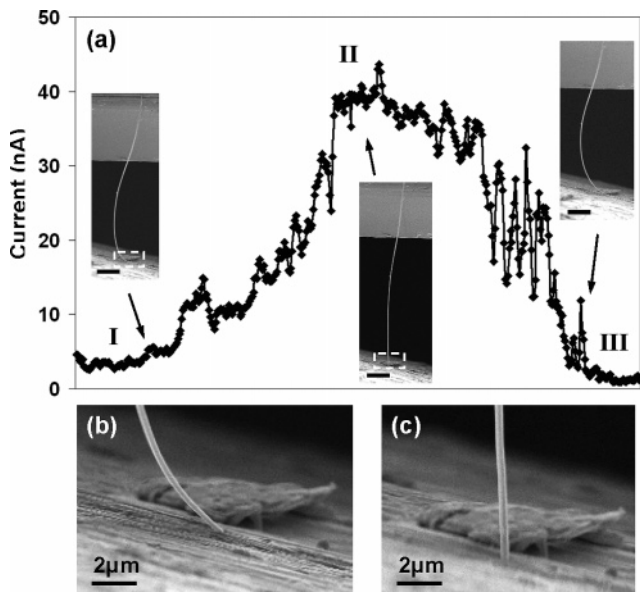
Figure 3. (a) Current variation with a continuous releasing and bending process of the ZnO nanowire; insets are the three typical bending cases in stage I, II, and III, respectively; the scale bar represents 10 μm. (b, c) SEM images of the contacting point between the ZnO nanowire tip and the tungsten needle surface when the nanowire was bent and released, showing no sliding and no losing.

Figure 4. Schematic diagrams showing the mechanisms responsible to the conductance change. (a) A finite element simulation of the strain distribution along the ZnO nanowire when it is bent. (b) The carrier trapping effect. (c) The creation of a charge depletion zone.

the $I-V$ curves indicates good Ohmic contacts at both ends of the NW.[20] Among the five bending cases, the current dropped significantly with the increase of bending (curves b–e in Figure 2f), indicating the decreased conductance with the increased strain.

This phenomenon was further confirmed by continuously changing the bending curvature under SEM observation. In this measurement, the applied voltage was fixed at +5 V and the current was continuously recorded while the ZnO NW was pulled back from large bending to almost straight and then pushed down again. The current variation is shown in Figure 3a. When the NW was under significant compression, the current was only ~5 nA (stage I in Figure 3a). As the NW was slowly released and recovered its straight shape, the current increased continuously with the decreasing of bending curvature, and the current was stabilized at ~40 nA (stage II in Figure 3a). The current dropped immediately when the NW was bent further (stage III in Figure 3a). This reveals a reversible sequence that the current passing through the ZnO NW at a fixed voltage was approximately inversely proportional to its bending curvature. Higher magnification SEM images were also taken at the contacting point when the NW was straight and highly bent (white rectangular boxes in the inset images of Figure 3a), and the corresponding images are shown in panels b and c of Figure 3, respectively. It can be clearly observed that the NW was firmly attached to the tungsten needle surface without sliding, indicating the contacting was well retained during bending process and should not cause any change in contact resistance.

We now examine the mechanisms that are responsible for the change of conductance. When a semiconductor crystal is under strain, the change in electrical conductance is
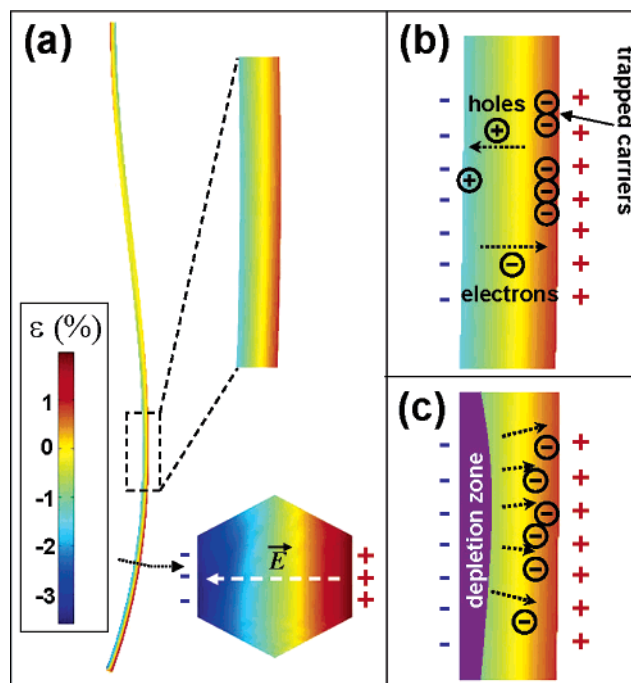
normally referred to as the piezoresistance effect, which is usually caused by a change in band gap width as a result of strained lattice.[21,22] The change of resistance is given by

$$\delta\rho/\rho = \pi \, \delta l/l \qquad (1)$$

where ρ is the resistance, l is the original length, and π is the piezoresistance coefficient. This equation is for a crystal that is subjected to a homogeneous strain. Practically, in order to achieve a detectable change in resistance, a semiconductor strain sensor is normally affixed to the surface of the object, of which the strain is to be measured. The built up strain in the object is equivalently picked up by the semiconductor slab, which is either stretched or compressed homogeneously through its entire volume.[23]

However, in our experiment, the strain in the bent ZnO NW is not homogeneous across its cross section. We have used finite element to simulate the strain distribution in a bent NW with hexagonal cross section. The calculation was for a NW with aspect ratio of 100. As shown in Figure 4a, after being subjected to bending, the inner arc surface of the NW is compressed ($\epsilon = \delta l/l < 0$), the outer arc surface is stretched ($\delta l/l > 0$), and area close to the center of the NW is strain free. This means that, across the cross section, δl varies linearly from the maximum negative value to the maximum positive value. Moreover, the total piezoresistance of the NW is an integration of eq 1 across the NW cross section and its length. As discussed above, the total piezoresistance of the bent NW is close to zero under the first-order approximation because of the nearly antisymmetric distribution of the strain across the width of the NW.

Therefore, the change in resistance of the NW as a result of bending is negligible. This result, however, cannot explain the experimentally observed result presented in Figures 2 and 3 that the resistance increased by a factor of ~7 after bending!

We now propose possible mechanisms for explaining the observed phenomenon. It is important to point out that ZnO is a material that simultaneously has semiconducting and piezoelectric properties. It is worth examination of the coupling between the two properties. Early in 1970, a 75% decrease in in-plane conductance of a semiconducting Si slab was observed when it was sandwiched between two pieces of piezoelectric PZT crystals that were busted by an ac power across the thickness.[24] The drop in the conductance of Si in the direction transverse to the propagation direction of the elastic wave in PZT was attributed to the trapping of free carriers at the surfaces of the silicon plate. This is a result of coupling between a semiconductor Si crystal and a PZT piezoelectric crystal. This coupling effect can now be achieved in a single ZnO NW due to its semiconducting and piezoelectric dual properties. On the basis of this discussion, a possible mechanism about the bending induced conductance change is suggested in parts b and c of Figure 4.

We have recently shown that a bent ZnO NW can produce a positively charged and negatively charged surface at the outer and inner bending arc surfaces of the NW due to the stretching and compression on the surfaces, respectively.[8] The charges are induced by a piezoelectric effect, and the charges are static and nonmobile ionic charges. The local electric field is $E_p = \epsilon/d$, where d is the piezoelectric coefficient. Thus a small electric field would be generated across the width of the ZnO NW, as shown in the cross-section image of the NW in Figure 4a. Upon the build up of the electric field, two possible effects can be proposed to account for the reduction of the NW's conductance: carrier trapping effect and the creation of a charge depletion zone.

Similar to the aforementioned Si-PZT system, when the piezopotential appears across the bent NW, some free electrons in the n-type ZnO NW may be trapped at the positive side surface (outer arc surface) and become nonmovable charges, thus lowering the effective carrier density in the NW (Figure 4b). On the other hand, even if the positive potential side could be partially neutralized by the trapped electrons, the negative potential remains unchanged. Hence, the piezo-induced electric field is retained across the width of the NW. This situation is similar to the case of applying a gate voltage across the width of the ZnO NW as for a typical NW FET. The free electrons will be repulsed away by the negative potential and leave a charge depletion zone around the compressed side, as shown in Figure 4c. Consequently, the width of the conducting channel in the ZnO NW becomes smaller and smaller while the depletion region becomes larger and larger with the increase of the NW bending. The two effects presented in parts b and c of Figure 4 are likely to contribute to the dramatic drop of the conductance of the ZnO NW with the increase of bending. The maximum width that the depletion zone can develop is up to the strain-free plane (close to central axis of the NW)
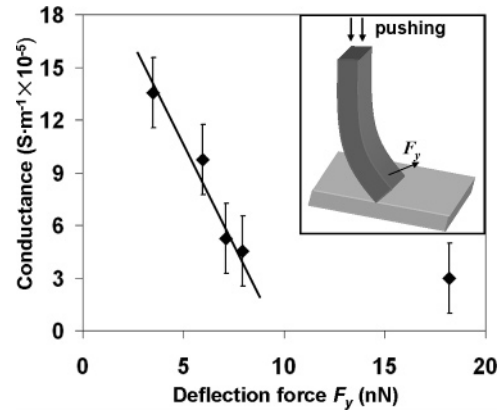
Figure 5. A plot showing the relationship between the ZnO nanowire conductance as PE-FET and the deflection force derived from the experimental data, demonstrating a nanoforce or nanopressure sensor using a single nanowire. Inset is the schematic of the deflected NW

with consideration of the piezoelectric field, which naturally sets an upper limit to the effect contributed by the depletion charges.

The structure shown in Figure 4 is the working principle of a FET except that the gate voltage was produced by a piezoelectric effect. Therefore, the single ZnO across two Ohmic contacts is a piezoelectric field effect transistor (PE-FET), which is a unique coupling result of the semiconducting and piezoelectric properties of ZnO.

Since the bending curvature of the NW is directly related to the force applied to it, a simple PE-FET force/pressure sensor is realized. The important step for calibrating the force/pressure sensor is how to quantitatively determine the force applied to the NW. As shown schematically in the inset in Figure 5, when the NW is pressed vertically, under small deflection angle approximation, the NW is deflected mainly due to the transverse force F_y and the bending shape of the NW is given by[25]

$$\frac{d^2 y}{dx^2} = \frac{F_y (L - x)}{YI} \tag{2}$$

where Y is the bending modulus, I is the momentum of inertia, and L is the total length of the NW. The shape of the bent NW is

$$y = \frac{F_y}{YI}\left(\frac{1}{2} Lx^2 - \frac{1}{6} x^3\right) \tag{3}$$

At the tip of the NW ($x = L$), the maximum deflection of the NW is

$$y_m = \frac{F_y L^3}{3YI} \quad \text{or} \quad F_y = \frac{3YI y_m}{L^3} \tag{4}$$

The bending modulus of ZnO NWs has been measured to be 109 GPa according to our previous data,[26] and I was calculated to be 6.62×10^{-28} m^4 for this particular NW. y_m

was measured from the SEM images. Since the SEM image is a projection of the 3D structure, in order for an accurate measurement, the bending curve should be parallel to the projecting screen. Considering this effect, the tungsten needle surface was tilted 15° to the right-hand side and the initial bending was achieved by lateral movement of the NW instead of directly pushing downward. After parallel bending of the NW, the stage was then pushed downward to achieve further bending, which can be kept in the same plane. Since there are nonlinear $I-V$ characteristics, the conductance was determined by the current measured at a constant 5 V potential. The total force versus conductance was plotted in Figure 5. At small bending, the decrease of conductance was almost linear to the bending force.

With the increase of bending at higher transverse force (17 nN), the dropping tendency of the conductance was reduced. This can also be understood from the two processes illustrated in Figure 4. At the beginning of bending, both contributions from the carrier trapping effect and the depletion zone increased with the bending curvature, thus producing a quick drop of the conductance. However, unlike the normal gate-controlled FETs, there was a positive potential on the outer side of the NW, which increased simultaneously with the negative potential at the inner side during the bending. The depletion region cannot extend beyond the neutral plane of the NW to the positive potential side. Thus, when the NW was bent to a significant degree, the piezoelectric field could not increase the size of the charge depletion zone and, hence, cannot reduce the size of the conduction channel.

It must be pointed out that the calculations in eqs 3 and 4 are for a NW that is subject to a small bending. The nonlinear effect has to be included if the degree of bending is large. This may cause significant change in the calibration of the measured force at larger applied forces. For practical application as force sensors, the measurements are recommended to be carried out under small deflections. For the data shown in Figure 5, the first four data points are most reliable for calibrating the sensor performance.

In summary, we have directly observed a decrease of the conductance of a single ZnO NW with increasing its elastic bending deformation by in situ manipulation and measurements in a SEM chamber. A new type of device, a piezoelectric field effect transistor (PE-FET) composed of a ZnO NW bridging two Ohmic contacts, has been demonstrated, in which the source to drain current is controlled by the bending of the NW. A possible explanation of this phenomenon is suggested to associate with the unique semiconducting and piezoelectric coupling effect of ZnO. Although the details of the process could be rather complex, we suggest that the carrier trapping effect and the creation of a charge depletion zone may be the two sources that are likely accounting for the reduced conductance. The PE-FET has been demonstrated as a force sensor for measuring forces in the nanonewton range and even smaller with the use of smaller NWs. An almost linear relationship between the bending curvature and the conductance was found at small bending regions, demonstrating the principle of nanowire-based nanoforce sensors.

References

(1) *Nanowires and Nanobelts Materials, Properties and Devices Nanowires and Nanobelts of Functional Materials Volume II*; Wang, Z. L., Ed.; Kluwer Academic Publishers: Norwell, MA, 2003.
(2) Wang, Z. L. *J. Phys.: Condens. Matter* **2004**, *16*, R829−R858.
(3) Arnold, M.; Avouris, P.; Pan, Z. W.; Wang, Z. L. *J. Phys. Chem. B* **2003**, *107*, 659−663.
(4) Wang, X. D.; Summers, C. J.; Wang, Z. L. *Nano Lett.* **2004**, *4*, 423−426.
(5) Huang, M.; Mao, S.; Feick, H.; Yan, H.; Wu, Y.; Kind, H.; Weber, E.; Russo, R.; Yang, P. *Science* **2001**, *292*, 1897.
(6) Yu, C.; Hao, Q.; Saha, S.; Shi, L.; Yang, X.; Wang, Z. L. *Appl. Phys. Lett.* **2005**, *86*, 063101.
(7) Buchine, B. A.; Hughes, W. L.; Degertekin, F. L.; Wang, Z. L. *Nano Lett.* **2006**, *6*, 1155.
(8) Wang, Z. L.; Song, J. H. *Science* **2006**, *312*, 242−246.
(9) Özgür, Ü.; Alivov, Y. I.; Liu, C.; Teke, A.; Reshchikov, M. A.; Doğan, S.; Avrutin, V.; Cho, S.-J.; Morkoç, H. *J. Appl. Phys.* **2005**, *98*, 041301.
(10) Lieber, C. M. *MRS Bull.* **2003**, *28*, 486−491.
(11) Friedman, R. S.; McAlpine, M. C.; Ricketts, D. S.; Ham, D.; Lieber, C. M. *Nature* **2005**, *434*, 1085.
(12) Huang, Y.; Duan, X.; Cui, Y.; Lauhon, L.; Kim, K.; Lieber, C. M. *Science* **2001**, *294*, 1313−1317.
(13) Patolsky, F.; Lieber, C. M. *Mater. Today* **2005**, *8*, 20−28.
(14) Zheng, G.; Patolsky, F.; Cui, Y.; Wang, W. U.; Lieber, C. M. *Nat. Biotechnol.* **2005**, *23*, 1294−1301.
(15) Duan, X.; Huang, Y.; Cui, Y.; Wang, J.; Lieber, C. M. *Nature* **2001**, *409*, 66−69.
(16) Qian, F.; Gradecak, S.; Li, Y.; Wen, C.; Lieber, C. M. *Nano Lett.* **2005**, *5*, 2287−2291.
(17) Cui, Y.; Wei, Q.; Park, H.; Lieber, C. M. *Science* **2001**, *293*, 1289−1292.
(18) Pan, Z. W.; Dai, Z. R.; Wang, Z. L. *Science* **2001**, *291*, 1947−1949.
(19) Wang, X. D.; Wang Z. L., Unpublished results.
(20) Sze, S. M. *Physics of Semiconductor Devices*; John Wiley & Sons, Inc.: New York, 1981.
(21) Bridgman, P. W. *Phys. Rev.* **1932**, *42*, 858−863.
(22) Smith, C. S. *Phys. Rev.* **1954**, *94*, 42−49.
(23) Chui, B. W.; Kenny, T. W.; Mamin, H. J.; Terris, B. D.; Rugar, D. *Appl. Phys. Lett.* **1998**, *72*, 1388−1390.
(24) Fischler, C.; Zucker, J.; Conwell, E. M. *Appl. Phys. Lett.* **1970**, *17*, 252−254.
(25) Song, J. H.; Wang, X. D.; Riedo, E.; Wang, Z. L. *Nano Lett.* **2005**, *5*, 1954−1958.
(26) Zhou, J.; Lao, C. S.; Gao, P. X.; Mai, W. J.; Hughes, W. L.; Xu, N. S.; Wang, Z. L. *Solid State Commun.* **2006**, *139*, 222.

NL061802G